Supporting Information

Enhanced water permeability in nanofiltration membranes using 3D accordion-like MXene particles with random orientation of 2D nanochannels

Yanchao Xu [1a], Wentian Zhang [1a], Zhiwen Li[a], Liguo Shen[a], Renjie Li[a], Meijia Zhang[a], Yang Jiao[a], Hongjun Lin*[a], and Chuyang Y. Tang*[b]

[a] College of Geography and Environmental Sciences, Zhejiang Normal University, Jinhua, 321004, China

[b] Department of Civil Engineering, the University of Hong Kong, Hong Kong S.A.R., China

*Corresponding author. Tel.: +86 0579 82291275, Email address: hjlin@zjnu.cn; tangc@hku.hk

Figure S1 presents the size distribution of AMXene particle by analyzing SEM images using a “Image-J” software [1].

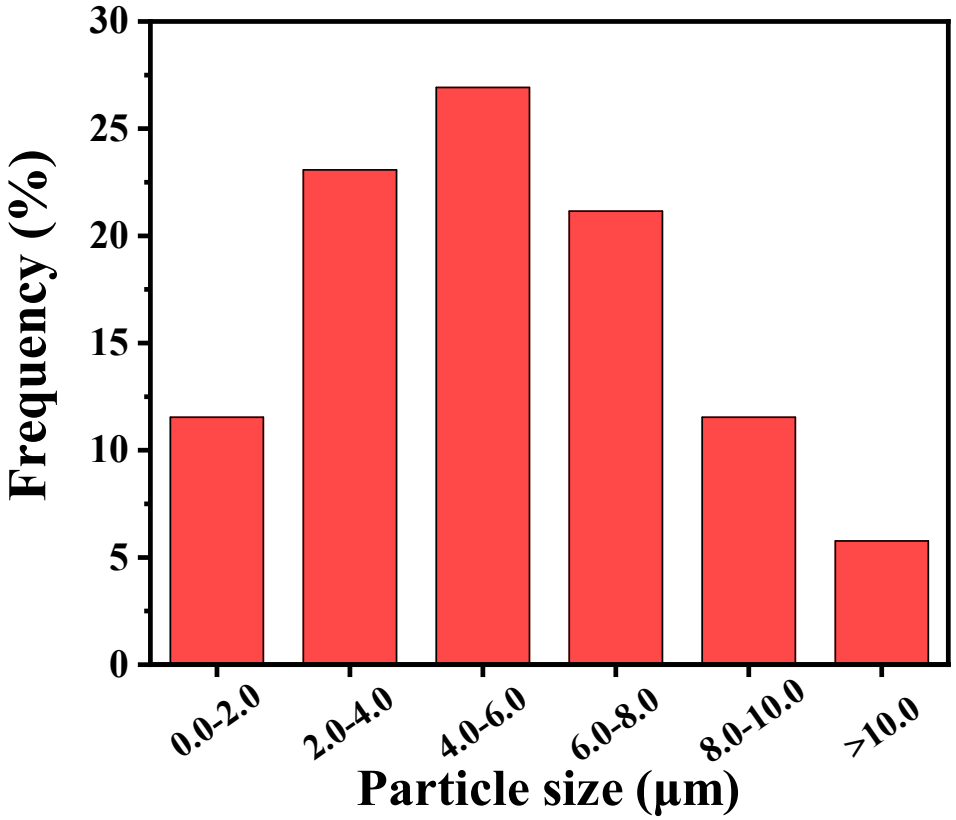

Fig S1. Size distribution of the AMXene particle.

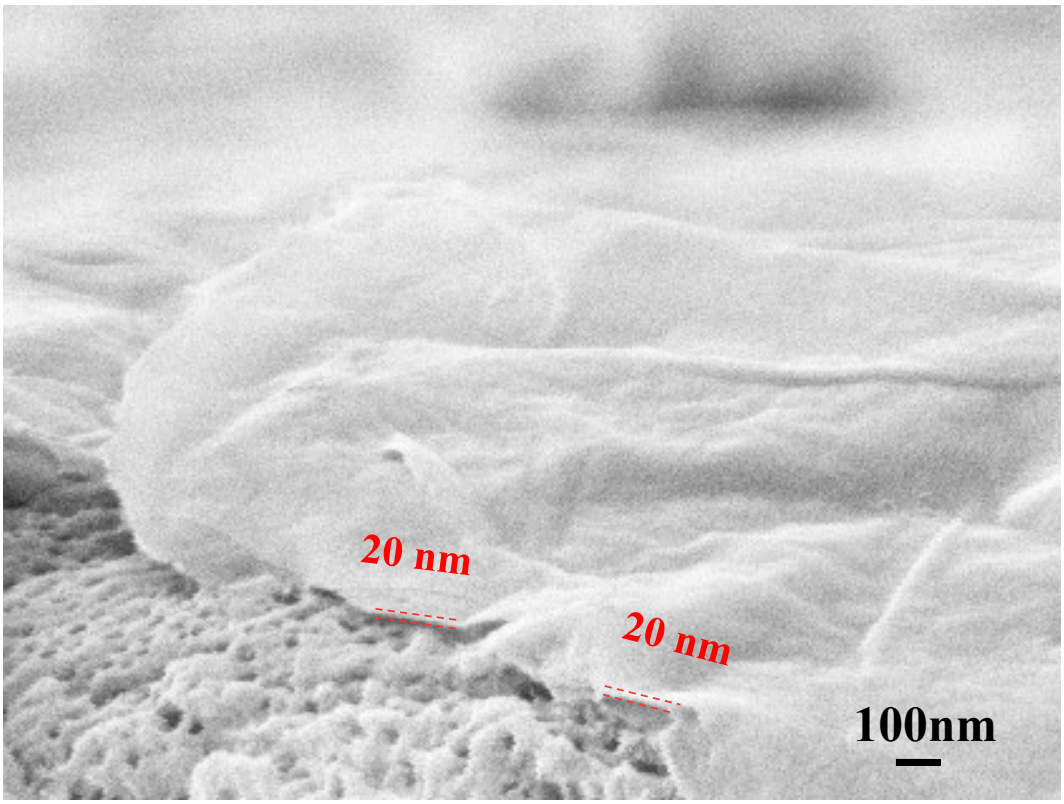

Fig S2. Cross-section SEM image of PVDF-MXene substrate.

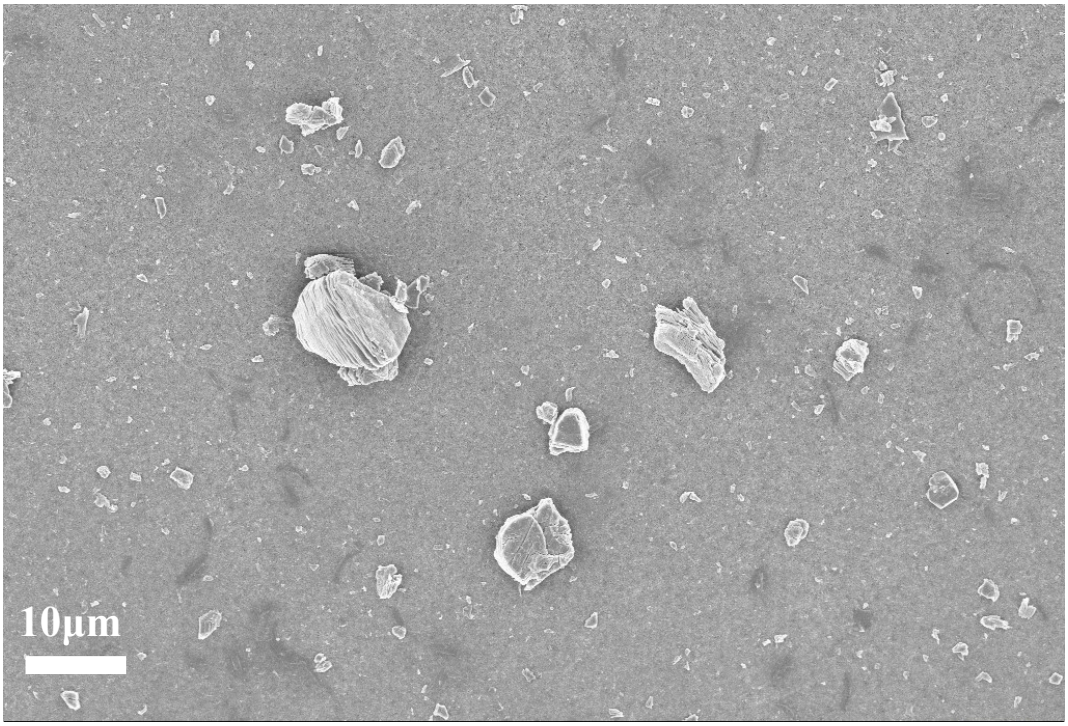

Fig S3. Surface SEM images of the PVDF-AMXene membrane.

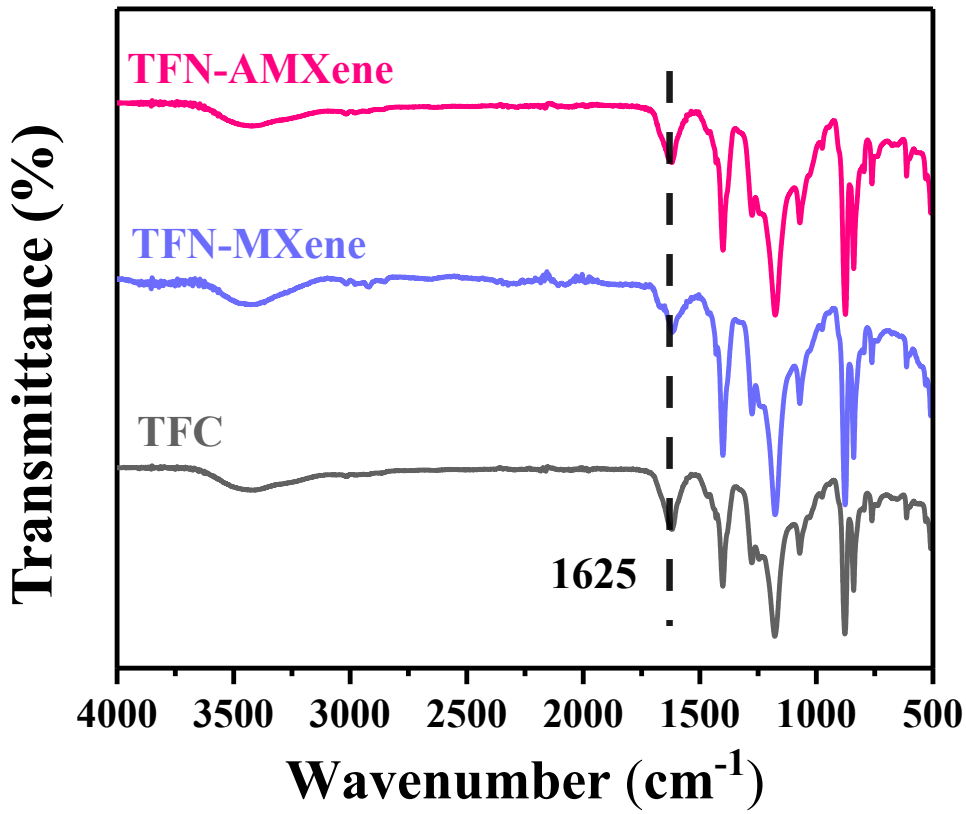

Fig S4. ATR-FTIR spectra of TFC and TFN membranes.

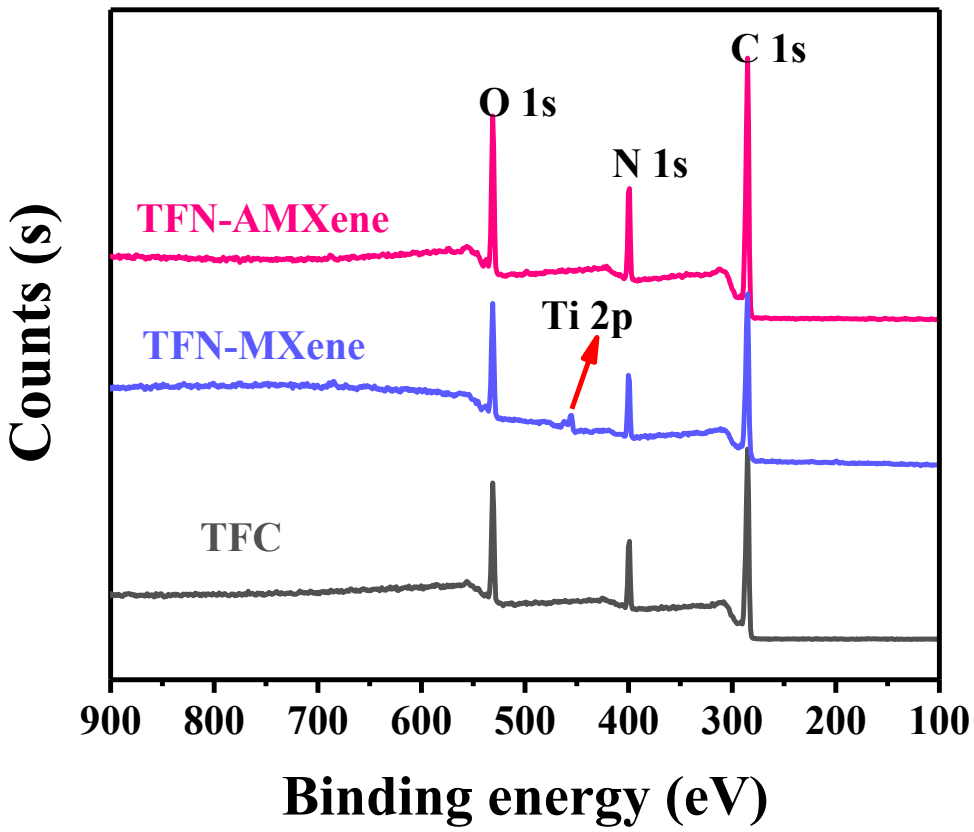

Fig S5. XPS spectra of TFC, TFN-MXene, and TFN-AMXene membranes.

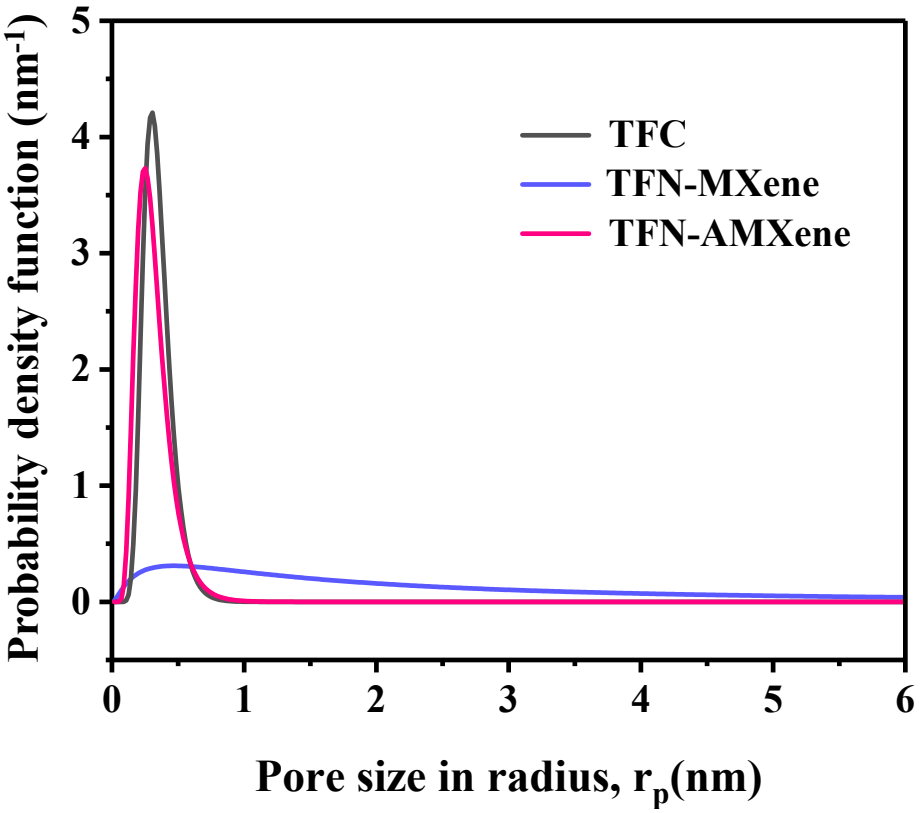

Fig S6. Pore size distributions of TFC, TFN-MXene, and TFN-AMXene membranes.

Membrane molecular weight cut off (MWCO) was calculated by using total organic carbon (TOC) analyzer (Shimadzu Corporation, Japan) to measure 200ppm PEG rejection. The molecule weights of PEGs used in this work were 200, 400, 600, 800, 1000, 6000, 10000, 20000, 70000, 100000 g mol^{-1}, respectively.

The membrane mean pore size and pore size distribution characterization were based on previous work[2, 3]. The relationship between solute rejection and diameter can be described by the Eq (S1):

$$R_T = \mathrm{erf}(\mathrm{y}) = \frac{1}{\sqrt{2\pi}} \int_{-\infty}^{\mathrm{y}} e^{-u^2/2} du \qquad \text{(S1)}$$

where

$$y = \frac{\ln r_s - \ln \mu_s}{\ln \sigma_g} \qquad \text{(S2)}$$

and R_T is the solute rejection, r_s represents the solution radius. μ_s is the geometric mean radius of solute at R_T = 50%, σ_g is the geometric standard deviation of μ_s, which defined as the ratio of the solute radius at R_T = 84.13% and R_T = 50%. In the log-normal probability graph, the

relationship between R_T and r_s can be described in a lineal formation:

$$F(\mathrm{R}_T) = A + B\ln r_s \quad \text{(S3)}$$

without regard to the hydrodynamic and steric hindrance between membrane pores and solute, μ_p (the mean effective pore radius) and σ_p (the standard deviation) can be substituted as the μ_s and θ_g. Therefore, based on the previous data, the pore size distribution is determined by the Eq (S4):

$$\frac{dR\left(d_p\right)}{dd_p} = \frac{1}{d_p \ln\sigma_p \sqrt{2\pi}} \exp\left[-\frac{\left(\ln d_p - \ln\mu_p\right)^2}{2\left(\ln\sigma_p\right)^2}\right] \quad \text{(S4)}$$

where d_p is the pore size in diameter.

The Stokes radii (m) of PEG were calculated based on the following Eq (S5):

$$r_s = 16.73\times10^{-12}\times MW^{0.557} \quad \text{(S5)}$$

where r_s represents the corresponding stokes radii of the PEGs and MW (g mol^{-1}) is the molecular weight of the PEGs.

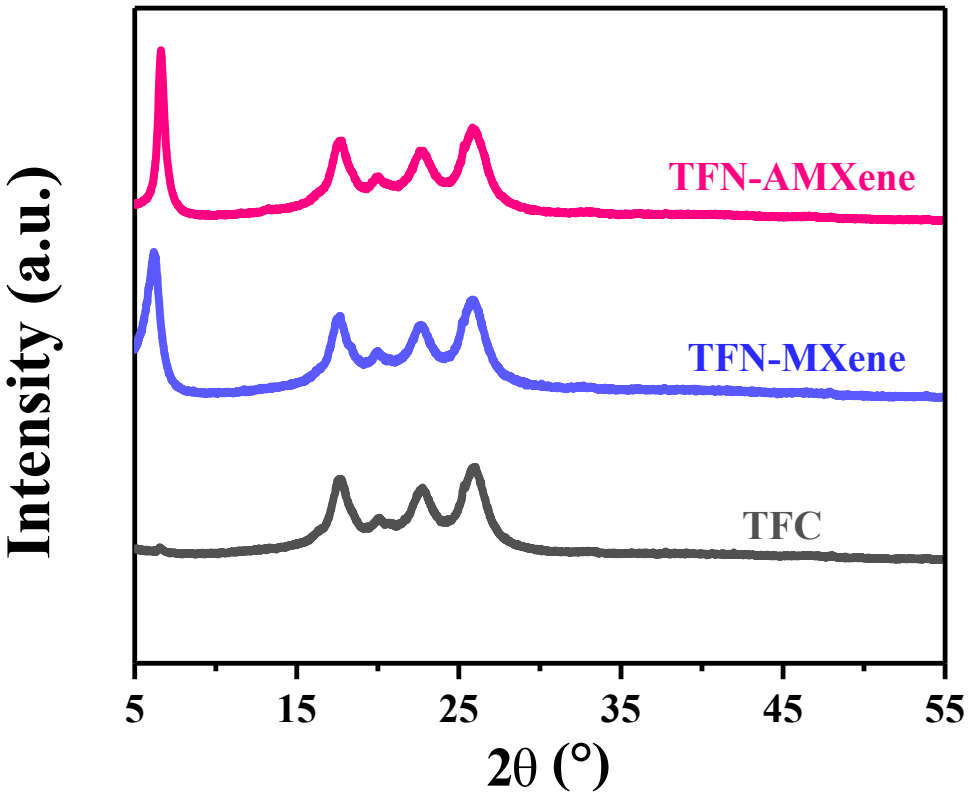

Fig S7. XRD pattern of TFC and TFN membranes.

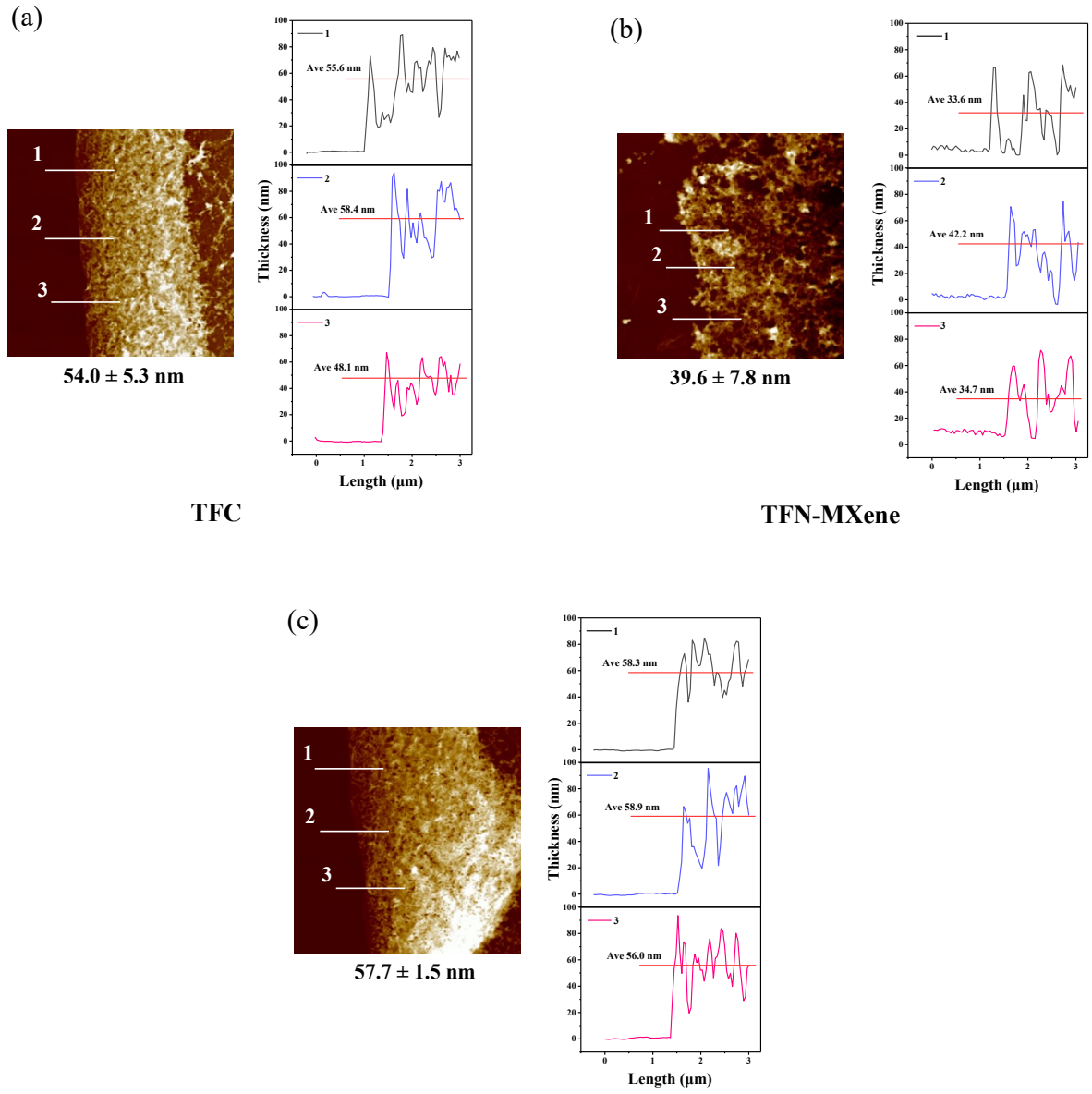

Fig S8. Thicknesses measured by cross-sectional AFM height scanning of a PA layer from (a) TFC, (b) TFN-MXene, and (c) TFN-AMXene membranes.

The TFC or TFN membrane was immersed into a DMF solution to dissolve the substrate and obtain a free polyamide layer, which was further immersed in a water solution and further transferred to a silica wafer. Then the silica wafer supported PA layer was dried and measured by cross-sectional AFM height scanning.

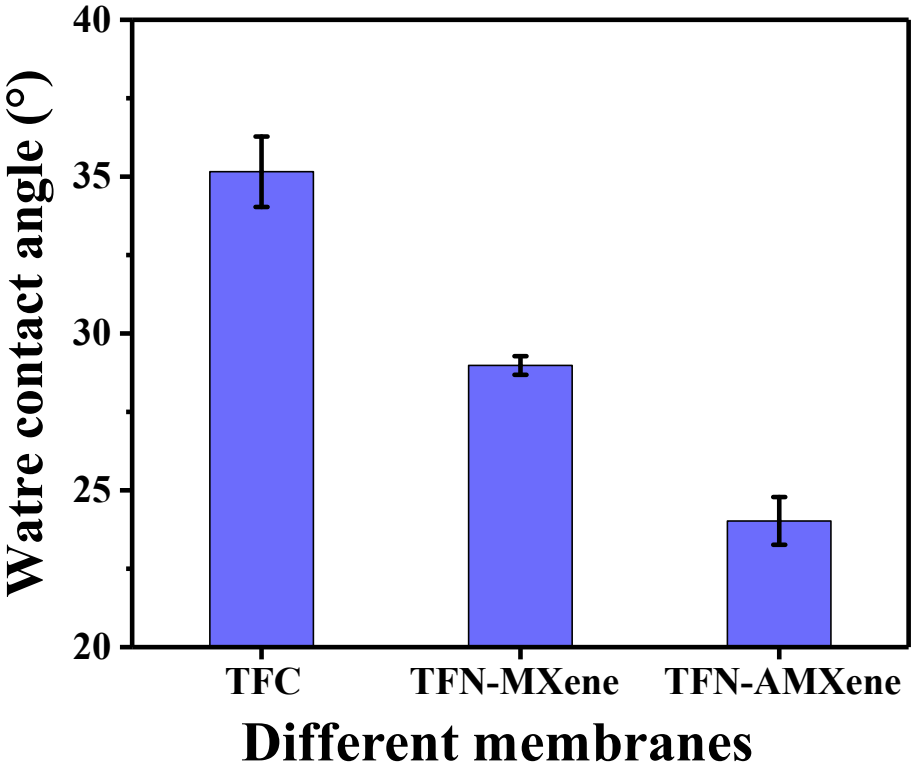

Fig S9. Water contact angles of different membranes.

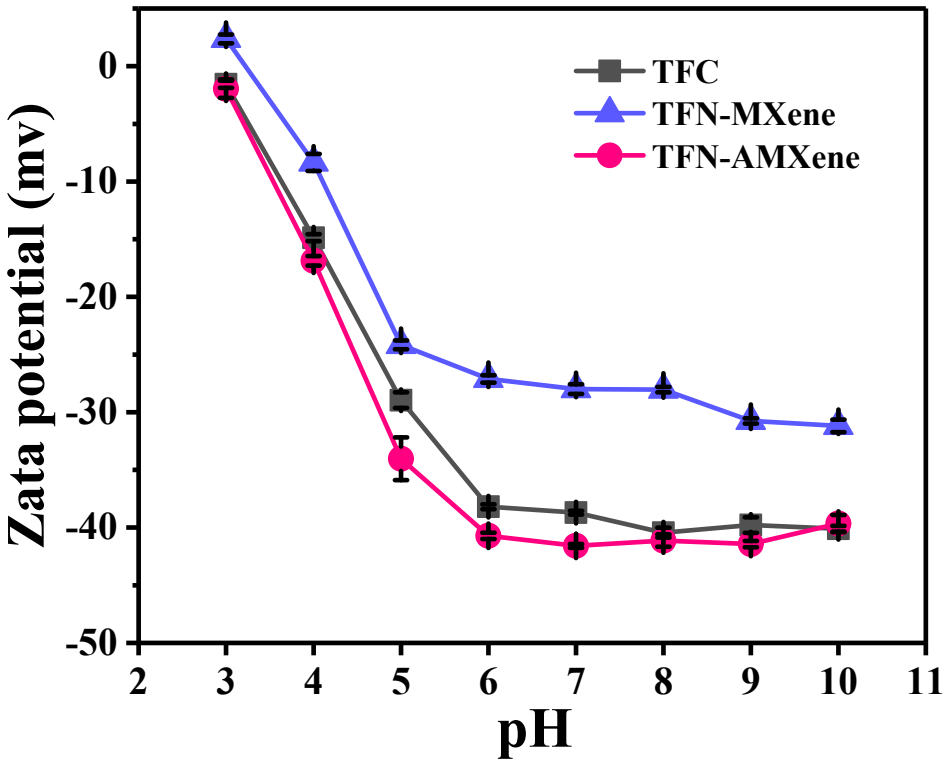

Fig S10. Zeta potentials of different membranes.

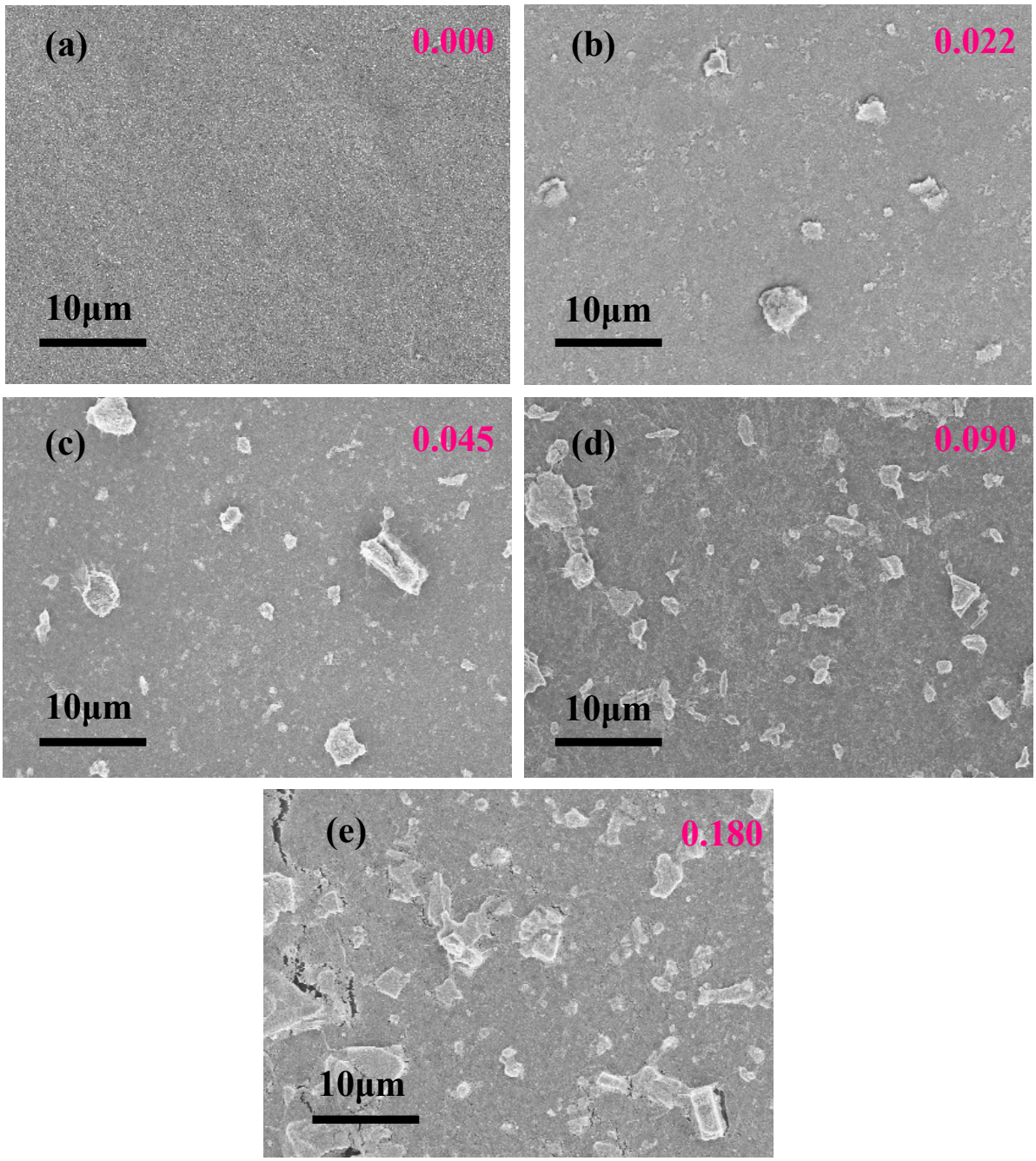

Fig S11. Surface SEM images of TFN-AMXene with different among of AMXene loading (mg/cm^2).

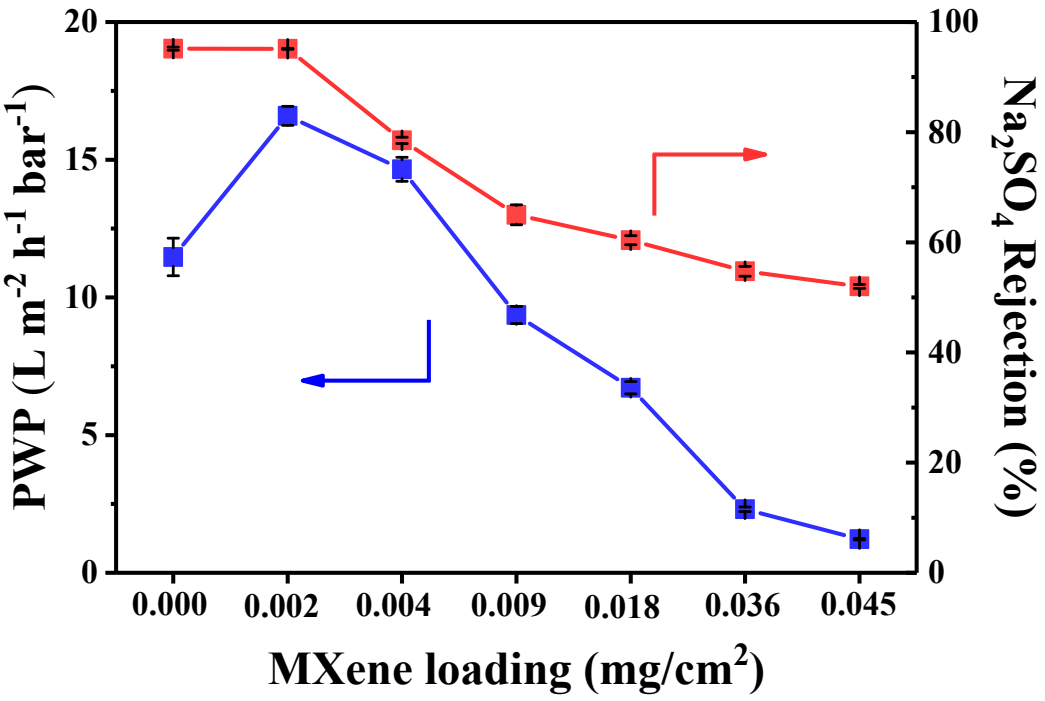

Fig S12. The effect of MXene loading on the separation performance of the TFN-MXene membrane.

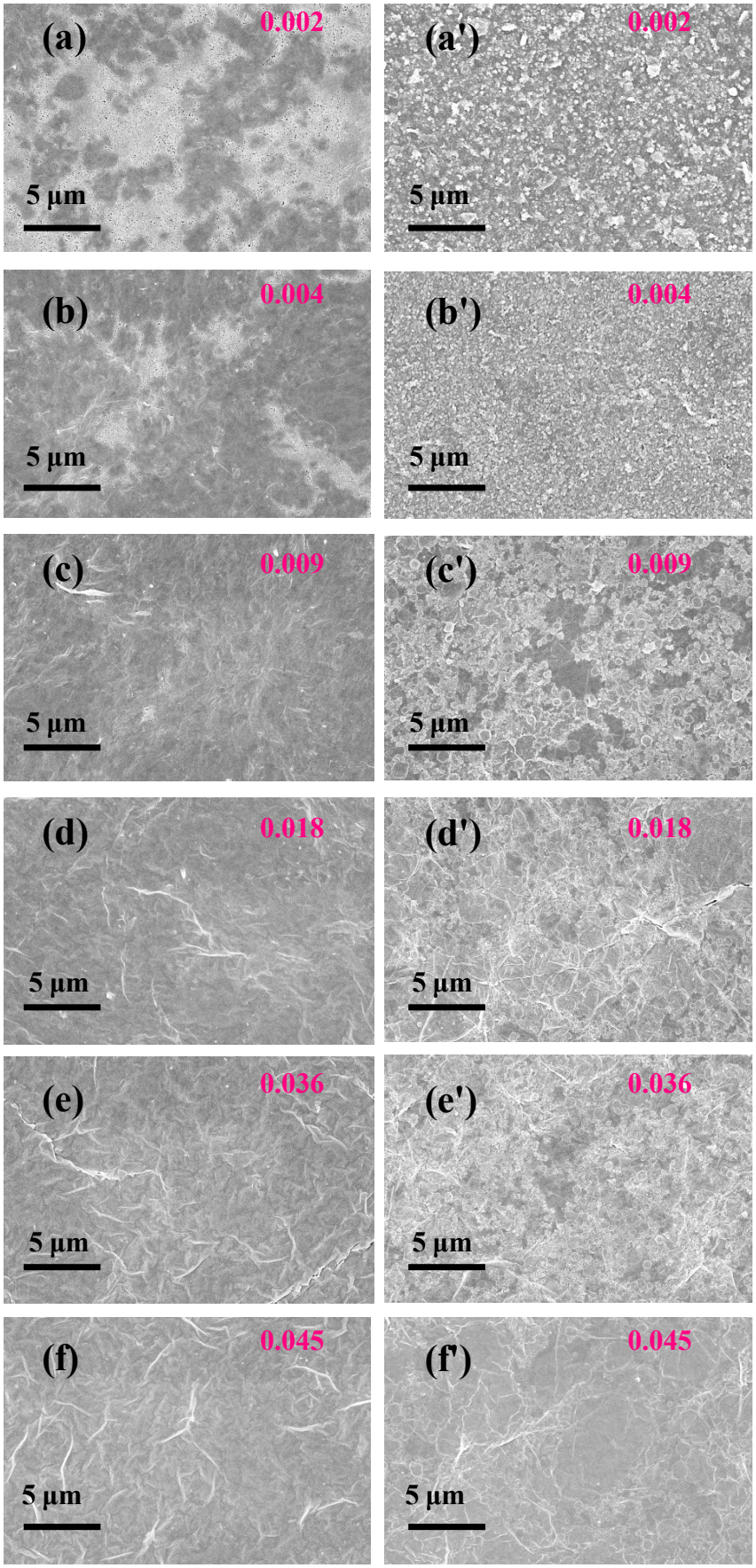

Fig S13. Surface SEM images of PVDF-MXene substrates (a-f) and the corresponding TFN-MXene (a'-f') prepared at different among of MXene loading (mg/cm^2).

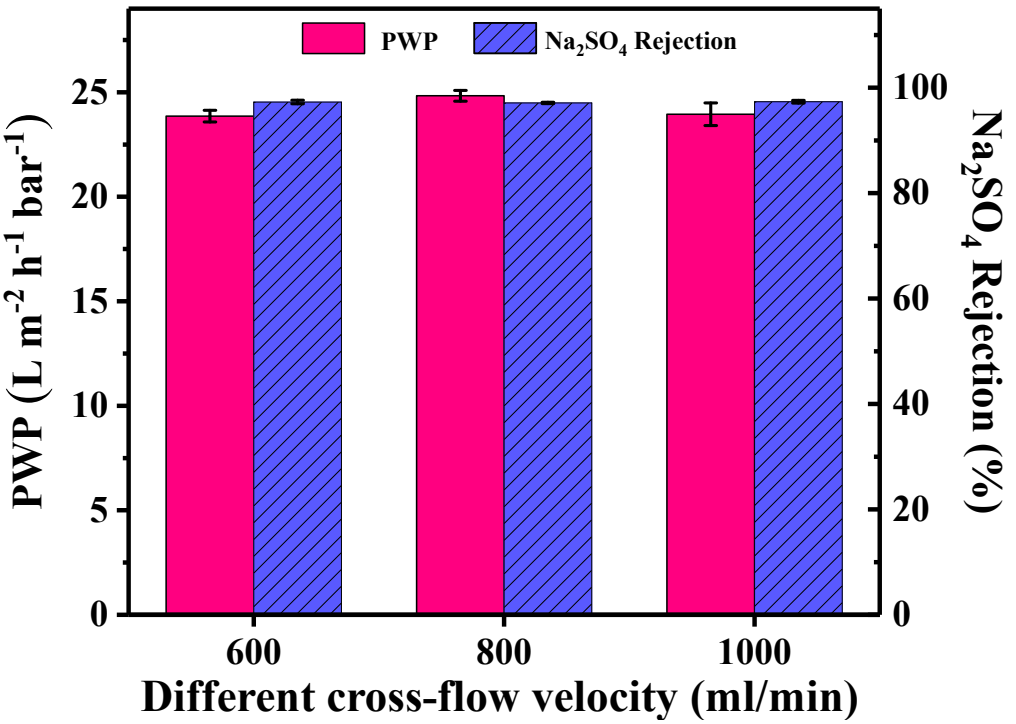

Fig S14. The performance of TFN-AMXene membrane under different cross-flow velocity

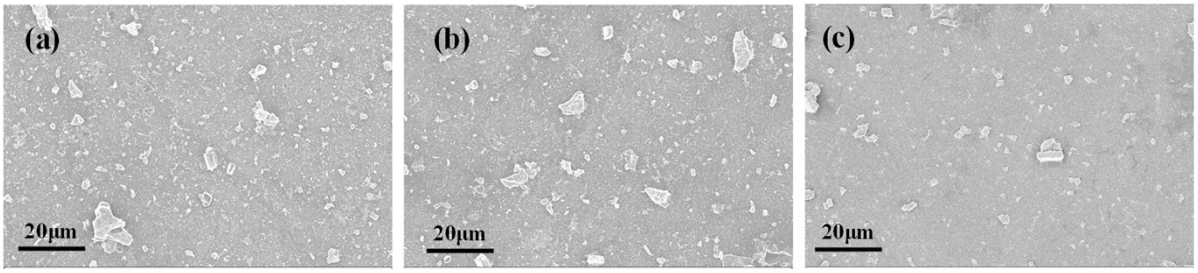

Fig S15. (a)-(c) Surface SEM images of the TFN-AMXene membrane after 2h filtration under 600, 800, 1000ml/min respectively.

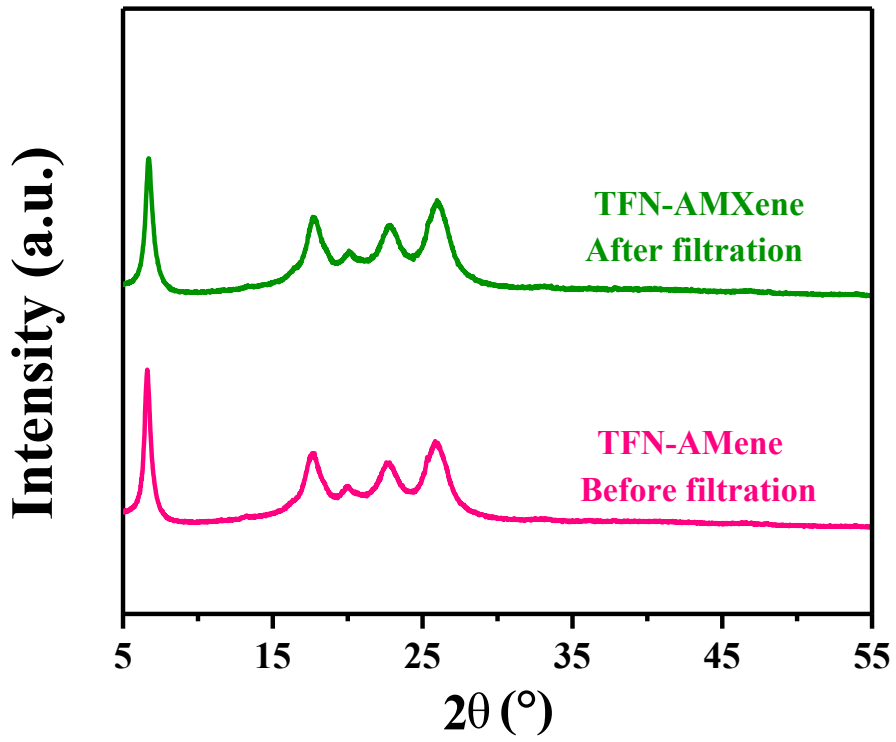

Fig S16. XRD patterns of TFN-AMXene membrane before and after filtration under 1000ml/min cross-flow velocity.

Table S1. Interlayer spacing of particles and membranes based on XRD results.

	2θ (°)	Interlayer spacing (nm)		2θ (°)	Interlayer spacing (nm)
MXene	6.8	1.29	AMXene	6.6	1.33
PVDF-MXene	6.3	1.40	PVDF-AMXene	6.6	1.33
TFN-MXene	6.3	1.40	TFN-AMXene	6.6	1.33

The interlayer spacing was determined from Bragg's law[4]:

$$2d \sin\theta = n\lambda \quad \text{(S6)}$$

where d is the crystal planar interlayer spacing (nm), θ is the X-ray beam incident angle, n is a positive integer (n = 1), and λ is the wavelength of the incident wave (λ = 0.154 nm).

Table S2. Elemental composition, O/N ratio and degree of cross-linking of TFC and TFN membranes

Membrane	Atomic concentration (%)					O/N ratio	Degree of cross-linking (%)
	C	N	O	Ti	F		
TFC	69.94	14.10	15.96	/	/	1.13	81.69
TFN-MXene	67.68	13.27	16.02	1.59	1.44	1.20	/ [a]
TFN-AMXene	70.70	14.11	15.19	/	/	1.07	89.04

[a] The cross-linking of the TFN-MXene membrane cannot be obtained since the MXene flakes also contain O element.

The cross-linking degree of polyamide can be calculated by the Eq S7[5]:

$$\text{Degree of cross-linking (\%)} = \frac{m}{m+n} \times 100 \quad \text{(S7)}$$

where m and n are the cross-linked and linear parts of the PA layer. The values of m and n can be evaluated based on O/N ratio obtained from XPS analysis using Eq S8:

$$\frac{O}{N} = \frac{3m+4n}{3m+2n} \quad \text{(S8)}$$

Table S3. Membrane surface roughness and surface area increase of membranes[6].

Sample	Rq (nm)	Surface area increase (%)
TFC	49.8	28.1
TFN-MXene	69.1	32.7
TFN-AMXene	116.0	48.9

Table S4. Zeta potentials under pH 7 and water contact angles of both MXene flakes and AMXene particles.

	MXene flake	AMXene particle
Zeta potential under pH 7 (mV)	-40.1 ± 1.4	-13.9 ± 0.8
Water contact angle (°)	25	< 10

The Zeta potential of MXene flakes and AMXene particles were measured by Malvern Zetasizer Nano ZS analyzer under pH 7.

To test the water contact angle of MXene flakes and AMXene particles, the MXene solution firstly dropped onto a clean slide, and the AMXene particles need to be laid on a slide and compacted. Both of them need to be dried for 30 minutes before testing and used in same amount.

References

1. Lu, Y.; Wang, R.; Zhu, Y.; Wang, Z.; Fang, W.; Lin, S.; Jin, J., Two-dimensional fractal nanocrystals templating for substantial performance enhancement of polyamide nanofiltration membrane. *Proceedings of the National Academy of Sciences* **2021,** *118*, (37).
2. Singh, S.; Khulbe, K. C.; Matsuura, T.; Ramamurthy, P., Membrane characterization by solute transport and atomic force microscopy. *Journal of Membrane Science* **1998,** *142*, (1), 111-127.
3. Cheng, X. Q.; Shao, L.; Lau, C. H., High flux polyethylene glycol based nanofiltration membranes for water environmental remediation. *Journal of Membrane Science* **2015,** *476*, 95-104.
4. Sun, Y.; Li, S.; Zhuang, Y.; Liu, G.; Xing, W.; Jing, W., Adjustable interlayer spacing of ultrathin MXene-derived membranes for ion rejection. *Journal of Membrane Science* **2019,** *591*, 117350.
5. Lai, G. S.; Lau, W. J.; Goh, P. S.; Ismail, A. F.; Tan, Y. H.; Chong, C. Y.; Krause-Rehberg, R.; Awad, S., Tailor-made thin film nanocomposite membrane incorporated with graphene oxide using novel interfacial polymerization technique for enhanced water separation. *Chemical Engineering Journal* **2018,** *344*, 524-534.
6. Tan, Z.; Chen, S.; Peng, X.; Zhang, L.; Gao, C., Polyamide membranes with nanoscale Turing structures for water purification. *Science* **2018,** *360*, (6388), 518-521.